microbiology research

MDPI

Article

Molecular Networks Underlying Wheat Resistance and Susceptibility to *Pyrenophora tritici-repentis*

Larissa Carvalho Ferreira [1,2,*], Flavio Martins Santana [3] and Luis A. J. Mur [2]

[1] Department of Plant Pathology, Everglades Research and Education Center, University of Florida, Belle Glade, FL 33430, USA
[2] Department of Life Sciences, Aberystwyth University, Aberystwyth SY23 3DA, UK; lum@aber.ac.uk
[3] EMBRAPA Trigo, Rodovia BR-285 Km 294, Passo Fundo 99050-970, RS, Brazil; flavio.santana@embrapa.br
* Correspondence: larissacarvalhof@ufl.edu

Abstract

Pyrenophora tritici-repentis (*Ptr*), the causal agent of tan spot, is a necrotrophic fungus that represents a significant threat to wheat production worldwide. The development of resistant cultivars is limited by an incomplete understanding of wheat defence responses against *Ptr*. Here, weighted gene co-expression network analysis (WGCNA) was applied to RNA-seq data from resistant (Robigus) and susceptible (Hereward) wheat lines before and after *Ptr* infection to identify coordinated host responses. Eight co-expression modules were identified, three of which were linked to either resistance, susceptibility, or *Ptr* infection. The resistance-associated module was enriched with chloroplast ribosomal machinery genes (e.g., 50S ribosome-binding GTPase, L28, L6), and transcriptional regulators. This suggested that maintaining chloroplast function, coupled with large-scale transcriptional reprogramming, was important for resistance. The susceptibility-associated module indicated the high expression of post-transcriptional modifiers, including SGS3, RBX1, and SENPs. The *Ptr*-responsive module showed common responses in both genotypes and included several defence-related genes (nucleotide-binding domain leucine-rich repeat R-genes [NLRs], chitinases, beta-1,3-glucanases) and metabolic pathways, such as phenylpropanoid biosynthesis and nitrogen metabolism (phenylpropanoid ammonia lyase [PAL], cytochrome P450s, glutamine synthase, and ammonium transporters). These results define distinct and shared molecular networks that are linked to resistance and susceptibility, providing valuable candidate genes for functional validation that could ultimately be exploited to enhance wheat resilience against necrotrophic fungal pathogens.

Keywords: *Pyrenophora tritici-repentis*; tan spot disease; *Triticum aestivum*; necrotrophic pathogen; gene-gene network

Academic Editor: Hector M. Mora-Montes

Received: 28 May 2025
Revised: 29 October 2025
Accepted: 11 November 2025
Published: 15 November 2025

Citation: Ferreira, L.C.; Santana, F.M.; Mur, L.A.J. Molecular Networks Underlying Wheat Resistance and Susceptibility to *Pyrenophora tritici-repentis*. *Microbiol. Res.* **2025**, *16*, 242. https://doi.org/10.3390/microbiolres16110242

1. Introduction

Pyrenophora tritici-repentis (*Ptr*) is a necrotrophic fungus that causes the economically important tan spot (TS) disease of wheat [1–4]. Pathogenicity in *Ptr* strains is linked to the production of effectors such as ToxA, ToxB, and ToxC, which are recognised in sensitive wheat lines by Tsn1, Tsc2, and Tsc3, respectively, in an inverse gene-for-gene resistance model [5–8]. Whilst multiple resistance loci have been identified in wheat lines [9], the development of TS resistance in elite germplasm has been hampered by a lack of understanding of the underlying defences in (in)sensitive hosts to *Ptr* strains. As a result, farmers still rely on fungicides to reduce TS incidence and severity.

ToxA is a necrotising toxin produced by *Ptr* races 1, 2, 7, and 8 [10–12], but also by the wheat pathogens *Stagonospora nodorum* and *Bipolaris sorokiniana* [13–15]. Manning and collaborators [16–20] demonstrated that PtrToxA is rapidly internalised within 2 h post infection (hpi) in mesophyll cells and into chloroplasts, through the binding protein ToxABP1. This triggers the chloroplastic production of reactive oxygen species (ROS) in sensitive lines, resulting in cell death (9–18 hpi) and macroscopic necrosis by 18 hpi. Microarray analysis of sensitive leaves treated with ToxA revealed a wide expression of receptor kinases (eg. BAK1, CDPK and MAPK) and transcription factors (eg. WRKYs, EREBP), as well as defences ordinarily associated with resistance, such as pathogenesis-related (PR) protein expression and the biosynthesis of phenylpropanoids, salicylic acid (SA) and jasmonic acid (JA) [21,22]. A recent transcriptomic study in resistant and susceptible cultivars challenged with *Ptr* race 2 inoculum and ToxA infiltration showed differential responses between both cultivars, as delineated by the expression of chitinases, transporters, kinases, and permeases, among others [23]. Previously, we integrated transcriptomic and metabolomic data to assess the parental lines of a multi-parent advanced generation intercross (MAGIC) population to *Ptr* strains that produce ToxA [24–26]. We identified a TS susceptible line (Hereward) that developed extensive chlorosis and numerous coalescing lesions, leading to widespread necrosis, and exhibited transcriptome changes akin to these mentioned above. In contrast, the moderately resistant line (Robigus) exhibited markedly fewer lesions and limited symptom development to small necrotic flecks with minimal chlorosis. One means of resistance was linked to an early barrier-related defence involving the cytoskeleton, cell wall, and plasma membrane, as well as the possible absence of susceptibility factors. However, the underlying mechanism(s) governing a secondary resistance in Robigus, which suppresses disease even after *Ptr* penetrate the host, remain unknown.

To provide further insights into our wheat–*Ptr* pathosystems, here we adopt a network analysis approach to our transcriptomic data. Network analysis offers a robust method to study large-scale multidimensional biodata [27]. It has been successfully applied to disease prediction [28], ecology and evolution inference [29], and to study plant–microbe interactions [30,31]. Advancements in computational biology allow for in silico reconstruction and investigation of interactions between various biological entities, such as protein–protein interaction networks, gene co-expression/association/regulatory networks, and metabolic networks. In gene networks, each node is representative of genes, and their interactions are represented as edges, which can be weighted or unweighted. In a weighted network, all nodes are interconnected, and the strength of these relationships are designated by weight values that vary between zero and one. In contrast, in unweighted networks, the connectivity between nodes is binary (zero or one), indicating whether a pair of genes are connected or not [32]. Network reconstruction using weighted, as opposed to unweighted, can produce more robust outputs [32]. Validated methods for gene network reconstruction include supervised learning, correlation, a probabilistic graphical model and meta-prediction [33]. Correlation-based approaches, such as weighted gene co-expression network analysis (WGCNA) [34] have facilitated scientists exploiting network approaches to characterise a range of systems, including the plant's immunity [35].

In this study, we used the WGCNA approach on RNA-seq data from two wheat lines (TS-resistant: Robigus [Rob] and TS-susceptible: Hereward [Her]), following challenges with *Ptr* and mock-inoculated controls. The specific objectives of this study were to do the following: (i) identify gene co-expression modules associated with various forms of resistance, susceptibility, and *Ptr* infection; (ii) determine key candidate genes within these modules; and (iii) highlight pathways that could be targeted in future wheat–*Ptr* studies and breeding programmes.

2. Materials and Methods

2.1. Expression and Trait Data

Transcriptomics data from our wheat-tan spot transcriptomics study PRJNA836737 was download from Gene Expression Omnibus (GEO) database (https://www.ncbi.nlm.nih.gov/geo/; accessed on 19 October 2024). The dataset comprises 36 RNA-seq samples collected from two wheat lines, namely Robigus and Hereward (also referred as Rob and Her), collected at different hours post-inoculation (hpi) with a ToxA positive strain of *Ptr*. Genotype and treatment metadata were converted into binary numeric arrays to be used as inputs (Table 1). Count data were normalised using a variance stabilising transformation within the R package Deseq2 [36]. After quantile normalisation, the top 95% most variant probes (2114 transcripts) were selected for WGCNA.

Table 1. Metadata for RNA-seq samples and trait data.

Sample	Genotype	Treatment	hpi	Trait Data						
				Rob	RobM	RobI	Her	HerM	HerI	HerI_RobI
RIT0R1	Rob	Untreated	0	1	1	0	0	0	0	0
RIT0R2	Rob	Untreated	0	1	1	0	0	0	0	0
RIT0R3	Rob	Untreated	0	1	1	0	0	0	0	0
RMT0R1	Rob	Untreated	0	1	1	0	0	0	0	0
RMT0R2	Rob	Untreated	0	1	1	0	0	0	0	0
RMT0R3	Rob	Untreated	0	1	1	0	0	0	0	0
HIT0R1	Her	Untreated	0	0	1	0	1	0	0	0
HIT0R2	Her	Untreated	0	0	0	0	1	1	0	0
HIT0R3	Her	Untreated	0	0	0	0	1	1	0	0
HMT0R1	Her	Untreated	0	0	0	0	1	1	0	0
HMT0R2	Her	Untreated	0	0	0	0	1	1	0	0
HMT0R3	Her	Untreated	0	0	0	0	1	1	0	0
RMT48R1	Rob	Mock	48	1	1	0	0	0	0	0
RMT48R2	Rob	Mock	48	1	1	0	0	0	0	0
RMT48R3	Rob	Mock	48	1	1	0	0	0	0	0
HMT48R1	Her	Mock	48	0	0	0	0	1	0	0
HMT48R2	Her	Mock	48	0	0	0	0	1	0	0
HMT48R3	Her	Mock	48	0	0	0	0	1	0	0
RIT48R1	Rob	Inoculated	48	1	0	1	0	0	0	1
RIT48R2	Rob	Inoculated	48	1	0	1	0	0	0	1
RIT48R3	Rob	Inoculated	48	1	0	1	0	0	0	1
HIT48R1	Her	Inoculated	48	0	0	0	1	0	1	1
HIT48R2	Her	Inoculated	48	0	0	0	1	0	1	1
HIT48R3	Her	Inoculated	48	0	0	0	1	0	1	1
RMT96R1	Rob	Mock	96	1	1	0	0	0	0	0
RMT96R2	Rob	Mock	96	1	1	0	0	0	0	0
RMT96R3	Rob	Mock	96	1	1	0	0	0	0	0
HMT96R1	Her	Mock	96	0	0	0	1	1	0	0
HMT96R2	Her	Mock	96	0	0	0	1	1	0	0
HMT96R3	Her	Mock	96	0	0	0	1	1	0	0
RIT96R1	Rob	Inoculated	96	1	0	1	0	0	0	1
RIT96R2	Rob	Inoculated	96	1	0	1	0	0	0	1
RIT96R3	Rob	Inoculated	96	1	0	1	0	0	0	1
HIT96R1	Her	Inoculated	96	0	0	0	1	0	1	1
HIT96R2	Her	Inoculated	96	0	0	0	1	0	1	1
HIT96R3	Her	Inoculated	96	0	0	0	1	0	1	1

2.2. Construction of WGCNA

The selected transcriptional data were screened for outliers and missing values. After validation, co-expression modules were detected in 2114 transcripts, using the R package WGCNA version 1.7 [34]. The scale-free topology index was calculated for multiple powers, and we used the powerEstimate result and mean connectivity to select an appropriate soft threshold. A signed network was constructed, and modules were detected using a power of 16, mergeCutHeight of 0.25, and minModuleSize of 30, differently from the default parameters. Then, we calculated the first principal component of the gene expression matrix for each module (i.e., module eigengenes [ME]). To determine relationships between modules and the traits, person correlation (corr), and hierarchical clustering based on dissimilarity and adjacency were calculated between ME and the trait data on Table 1. Modules with significant correlations above 0.6 (p-value < 0.05) were selected for further analysis.

2.3. Intra-Modular Analysis and Identification of Hub Genes

Module membership (MM) of individual transcripts was defined as the correlation of the module eigengenes of interest and the gene expression profiles. Gene-trait significance (GS) was based on Pearson correlations between gene expression and trait data. To identify hub genes, we filtered transcripts with absolute values of GS > 0.6 and MM > 0.8 and also used the WGCNA built-in function chooseTopHubInEachModule(). The topological overlap matrix (TOM) computed for the genes in the selected modules was used to graphically represent the network, for which the visualisation was created in Cytoscape 3.8.2 [37]. To ease visualisation, we plotted only hub genes (nodes) and filtered edges with weight (TOM) > 0.1. The networks were arranged using the edge-weighted spring embedded layout, followed by the yFiles algorithm to remove overlaps.

2.4. Functional Annotation and Enrichment Analysis

The transcripts were aligned with the wheat reference genome IWGSC RefSeq v1.1 [38], and its functional annotation [39] was used to perform functional analysis. Gene ontology enrichment analysis was performed separately for each module using BiNGO [40]. The EnrichmentMap pipeline was then used to create a network visualisation of significantly enriched gene ontologies (Benjamini and Hochberg FDR corrected p-value < 0.05) [41].

3. Results

3.1. Global Co-Expression Network

WGCNA defined discrete modules of co-expressed genes in wheat leaves infected (I) with *Ptr* and mock-inoculated (M). The phenotypes of these interactions are described elsewhere [25] but are provided in Figure S1 for convenience. We selected a soft threshold of 16, as it fits a scale-free topology (R^2 = 0.87; Figure 1a) while maintaining a relevant mean connectivity between genes (Figure 1b). The targeted transcripts were clustered using an average linkage hierarchical clustering method, which indicated eight branches, representing distinct modules (Figure 1c, each module is coloured separately). Of the 2114 transcripts in the wheat-*Ptr* network, 2089 genes were assigned one of the eight modules, and the remaining were grouped into a "null module" (grey, not shown in Figure 1c). The number of genes in each module were 474 = turquoise, 440 = blue, 336 = brown, 319 = yellow, 288 = green, 89 = red, 75 = black, and 68 = pink (Supplementary Table S1). To assess whether the modules were biologically meaningful, we performed a functional enrichment analysis on the relationships between infection phenotypes and the expression data (Figure 2). To ease visualisation, expression data were consolidated into four groups: *Ptr*-inoculated and mock-inoculated samples from both lines (RobI, RobM, HerI, and HerM). Each module was significantly enriched with established pathways (Supplementary

Table S1). Highly co-expressed gene sets formed a network composed of 17 interconnected clusters and two subnetworks (Figure 2). Nodes within each cluster represented similar functions, suggesting the validity of the WGCNA network.

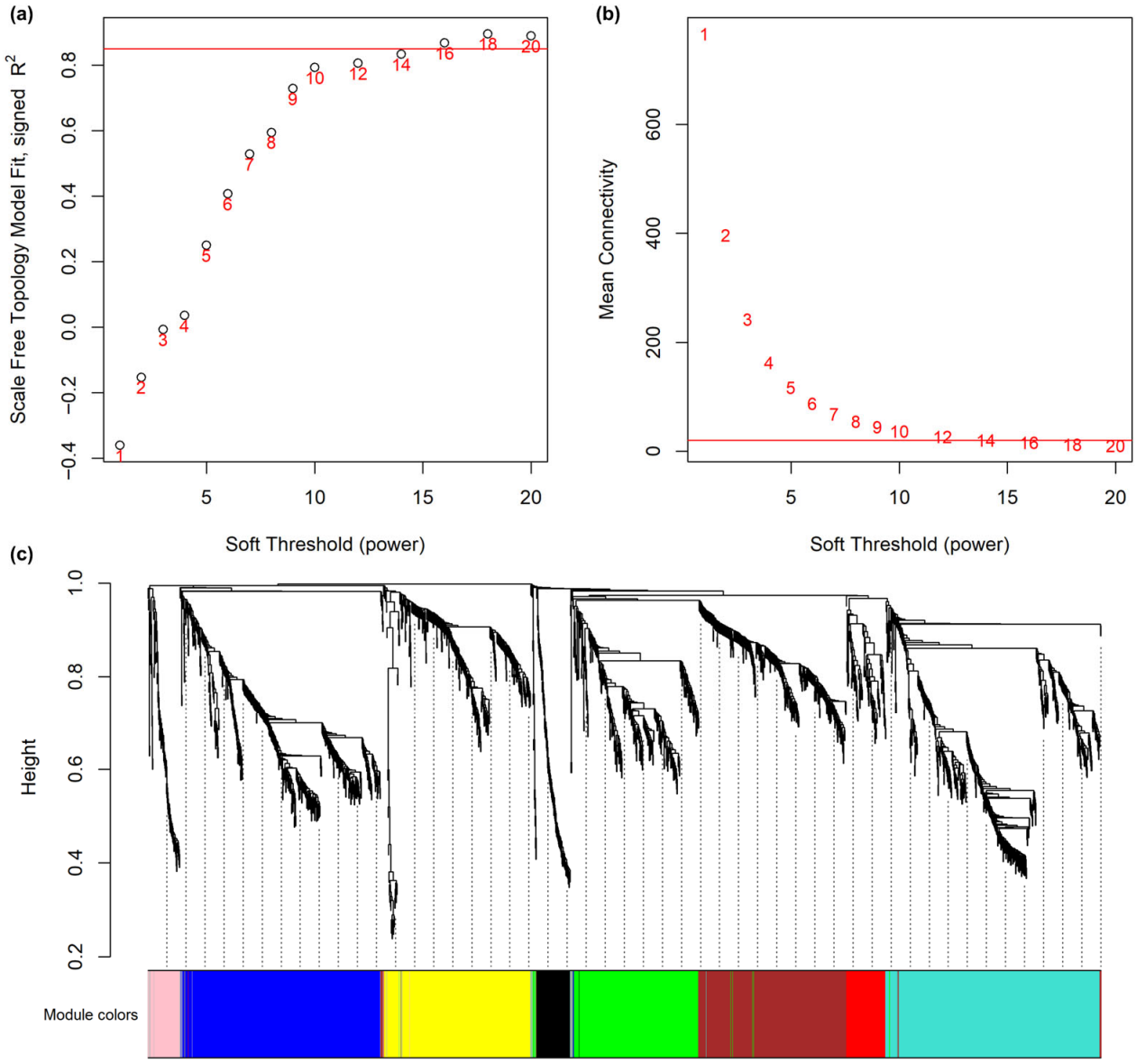

Figure 1. Network construction and module detection in the transcriptomes of wheat cultivars Robigus and Hereward challenged with *Pyrenophora tritici-repentis*. (**a**) The scale-free topology model fit index calculated for various soft-thresholding. The red line marks $R^2 = 0.85$, indicating the threshold selected for network construction. (**b**) Mean connectivity in function of various soft thresholding power. The red line indicates a mean connectivity of 20, which intersects with the chosen soft-thresholding power of 16. (**c**) Dendrogram of transcripts in the co-expression network produced by average linkage hierarchical clustering, based on topological overlaps. Each coloured cell represents a colour-coded module of co-expressing genes.

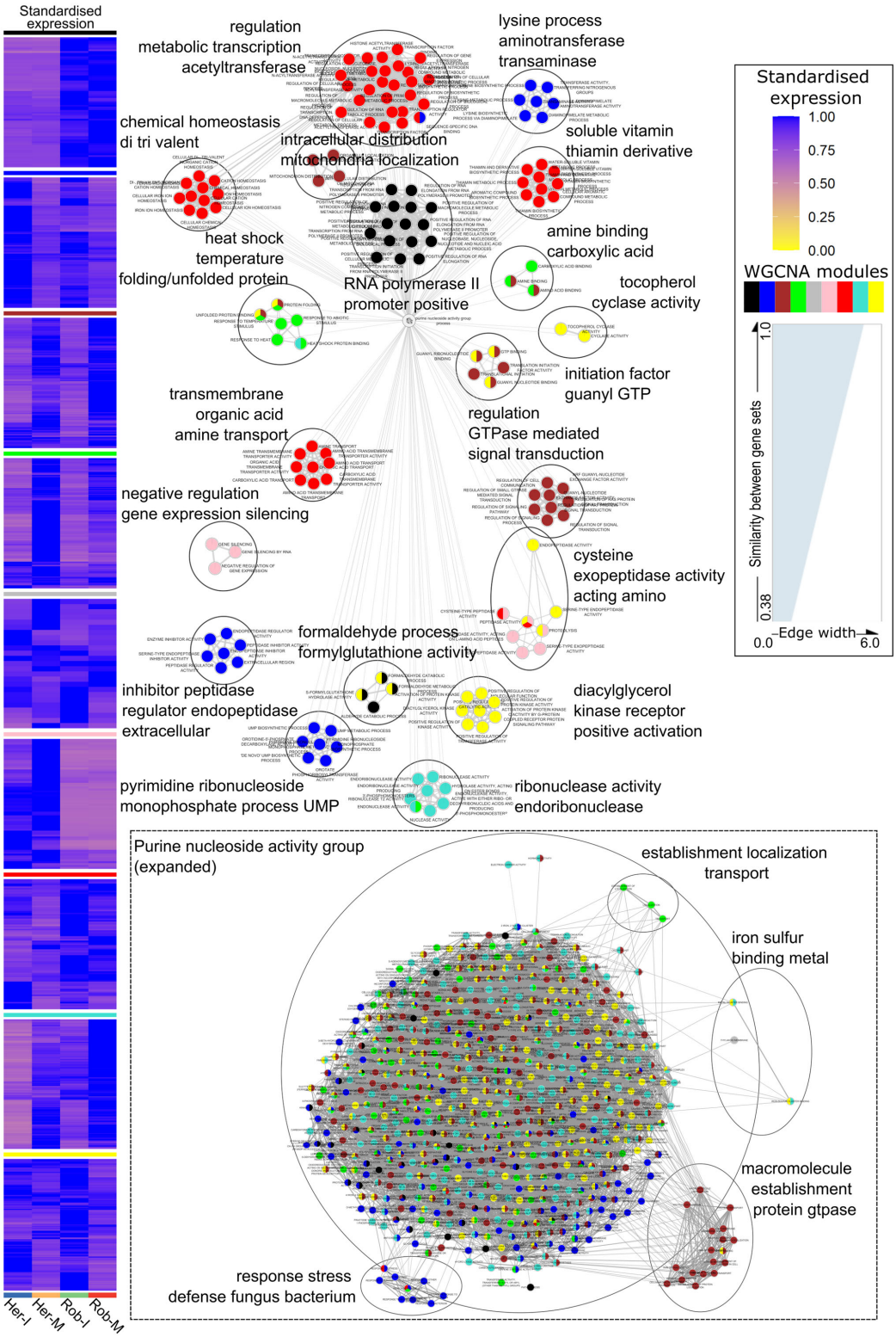

Figure 2. Gene ontology enrichment and expression patterns of all modules identified in transcriptomes of wheat cultivars Robigus (Rob) and Hereward (Her), challenged with *Pyrenophora tritici-repentis* (I) or mock-inoculated (M). Standardised expression profiles (0–1) for each module (colour bar above plots) are shown on the left for each of the four sample groups. Nodes represent enriched GO terms within modules (coloured), and edges indicate similarity between gene sets, with thicker edges denoting greater similarity. Nodes were clustered, and word cloud annotations summarise the major functional categories.

The largest cluster, including the purine nucleoside activity group, is linked to four subnetworks (establishment localisation, iron sulphur binding metal, macromolecule establishment protein GTPase, and response stress defence fungus bacterium) (Figure 2). Genes belonging to the turquoise module were highly expressed in the RobM samples and therefore are likely to reflect genotypic differences. These were related to endonuclease activity. The blue module represents a subnetwork of genes associated with the defence response to biotic stress, where expression is higher in *Ptr*-inoculated samples from both genotypes but more pronounced in Her. The three other clusters overrepresented by genes in the blue module play roles in (i) the lysine process and aminotransferase activity, (ii) pyrimidine ribonucleotide monophosphate process UMP and (iii) inhibitor peptidase regulator activity (subnetwork). The brown module encompassed two clusters and a subnetwork consisting of genes which were repressed in both genotypes following a challenge with *Ptr.* These were likely to represent common responses to fungal challenge, irrespective of the interaction being compatible or incompatible. These were associated with regulation of GTPase-mediated signal transduction, intracellular localization of mitochondria, and establishment of macromolecules. The yellow module represented genes that were significantly upregulated in Rob, but 14.4% were significantly repressed in Her when comparing *Ptr*- versus mock-treated samples. Functionally, these were associated with diacylglycerol, positive activation of kinase receptors, and tocopherol cyclase activity. The green network was repressed during infection in both genotypes and seemed to be linked to the suppression of stress responses, as indicated by the category "heat shock temperature folding/unfolded protein". Considering the red module, only 13 genes were significantly differentially expressed compared to M, with most being repressed in both genotypes. Genes in this module formed four distinct clusters and were involved in "soluble vitamin thiamine derivative", "regulation of metabolic transcription acyltransferase", "chemical homeostasis of trivalent", and "transmembrane organic acid amine transport". Perhaps most importantly, the black module consisted of genes whose expression was highly correlated with the resistance. Here, genes were functionally related to the regulation of RNA and transcription. The pink module represents a converse situation where genes are highly expressed in Her, following a challenge with *Ptr* and in controls. These were linked to "negative regulation gene expression silencing".

3.2. Module–Trait Relationships Reveal Common Responses Triggered by Ptr Infection in Resistant and Susceptible Genotypes

Next, we focused on modules that were correlated with the treatment groups, rather than selecting individual transcripts in each module. To do so, we carried out a correlation analysis between the trait data (Table 1) and the first principal component that was related to each module. Attempts to use correlation analysis for each discrete time point did not yield any significant results, so further analysis used consolidated data based on genotype/treatment rather than hpi. We found 11 significant positive correlations (p-value < 0.05) between traits' and modules' eigenvectors (in this case, related to variation in gene expression; "eigengenes"), and 13 negative correlations (Figure 3). The blue module was positively correlated (corr = 0.89) with inoculated samples from both genotypes (HerI_RobI). Conversely, the brown, green and turquoise modules were negatively correlated with HerI_RobI. These further indicated that blue and brown modules were linked to a common response to *Ptr* infection (Figure 2). Considering responses that were specific to Rob, the modules black and turquoise were positively correlated, and pink was negative, correlating with responses in this genotype. Separate correlation values for mock-inoculated samples from each genotype are shown in Figure 3. Genes in the black module are mostly correlated with the mock samples from Rob, with RobI data contributing to a correlation value of one, i.e., genes that are unaltered by *Ptr* infection. The

pink module was highly correlated to the control sample Her. Modules related with *Ptr* infection had higher correlation values with HerI (corr = 0.75) than with RobI (corr = 0.39). Despite several transcripts being more abundant in inoculated samples from Rob and Her (Figure 2), no modules had significant correlations greater than 0.8 that could allow for a tentative association with resistance or susceptibility (Figure 3). This was due to strict occupancy parameters used for module detection.

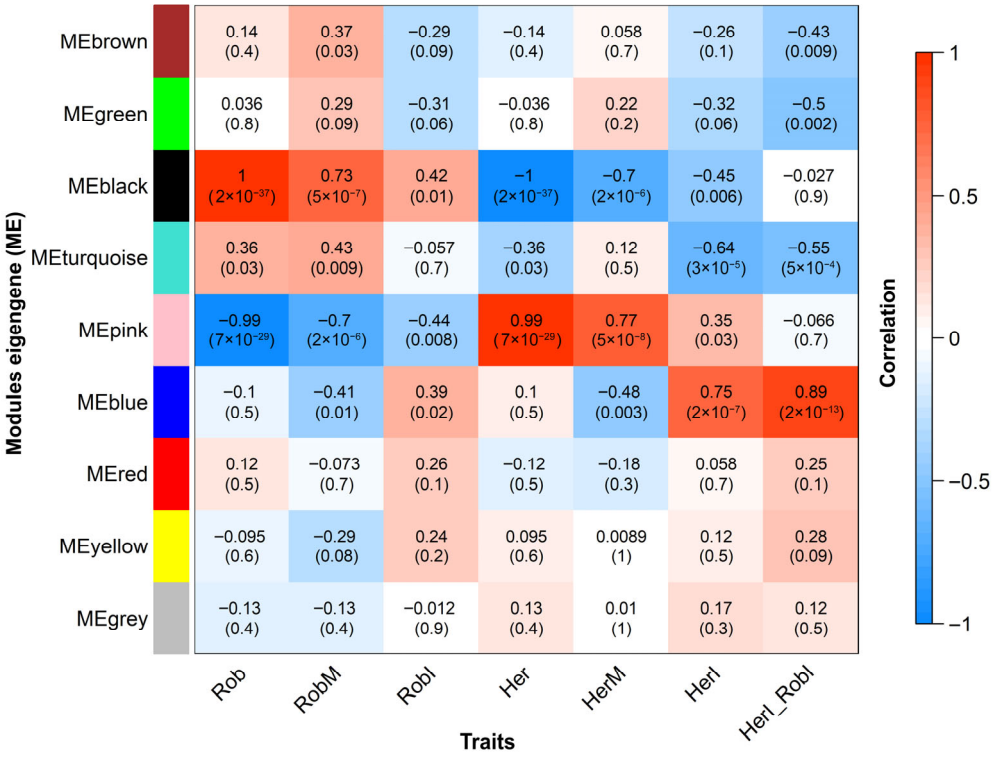

Figure 3. Module-trait correlations in transcriptomes of wheat cultivars Robigus and Hereward, challenged with *Pyrenophora tritici-repentis*. Each row corresponds to a module eigengene (ME), and each column to a trait. Each cell contains the corresponding correlation and *p*-value. The table is colour-coded by correlation, according to the colour legend.

To confidently investigate the mechanisms underlying the module–trait relationships, we concentrated on correlations >0.8 with at least one trait (i.e., black [unchanged in Rob following *Ptr* infection], pink [unchanged in Her following *Ptr* infection], and blue [common to both genotypes following *Ptr* challenge]). Initially, eigengene network analysis was used to quantify the relationship between the selected modules and traits and to assess if other correlated modules (meta-modules) could also be relevant. As indicated in Figure 4a, the black, pink, and blue modules clustered only with Rob, Her, and HerI_RobI, respectively. Further, the heatmap confirmed the distinctiveness of each module's eigengenes and confirmed the absence of meta-modules (Figure 4b). Then, the expression patterns of all the eigengenes in each module across the treatments were plotted (Figure 5). In line with predictions, eigengenes in the black module were overexpressed in samples from Rob compared to Her. The opposite expression profile was observed in eigengenes that form the pink module. Blue module transcripts were overexpressed in *Ptr*-treated samples collected at 48 and 96 hpi in both genotypes. Altogether, Figures 4 and 5 confirm the robustness of module detection and their relationships with *Ptr* and genotype traits.

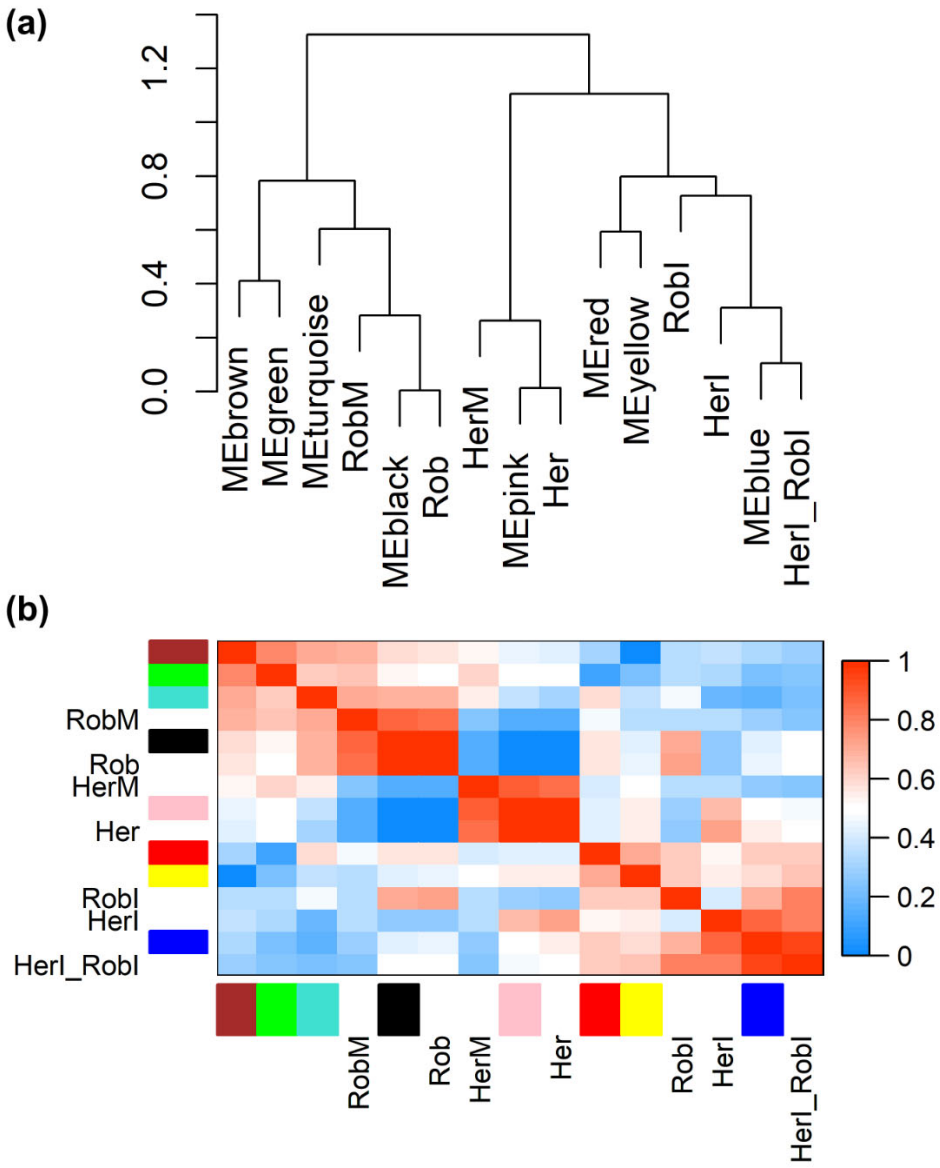

Figure 4. Visualisation of the eigengene network representing the relationships among the modules and traits in transcriptomes of wheat cultivars Robigus (Rob) and Hereward (Her), challenged with *Pyrenophora tritici-repentis*. Panel (**a**) shows a hierarchical clustering dendrogram of the eigengenes, in which the dissimilarity of eigengenes EI, EJ is given by 1−cor(EI,EJ). The heatmap in panel (**b**) shows the eigengene adjacency AIJ = (1 + corr(EI,EJ))/2.

3.3. Intramodular Analysis and Network Analysis of Hub Genes

We next considered how genes in each module could be contributing to their associated phenotypes. As a given gene may belong to more than one WGCNA module, we calculated module membership (MM) for all transcripts (Supplementary Table S2). This quantitative measure allowed us to identify nodes laying between modules, as well as those highly correlated to a module. Over half (57.33%) of black module transcripts had MM greater than 0.9, with all values ranging from 0.536 to 0.99. Genes with high module membership were less frequent in the pink (41.79%) and blue (37.95%) modules, with values as low as 0.328 and 0.245, respectively. Then, gene significance (GS) values were calculated to correlate gene expression and the traits data for the black, pink and blue modules (Supplementary Table S2). This showed a strong correlation (corr > 0.9) between gene significance and module membership in all three modules tested (Figure S2). Taken together, the gene

significance and module membership results indicate that transcript data can be used to confidently define the most important genes (hubs) contributing to each module.

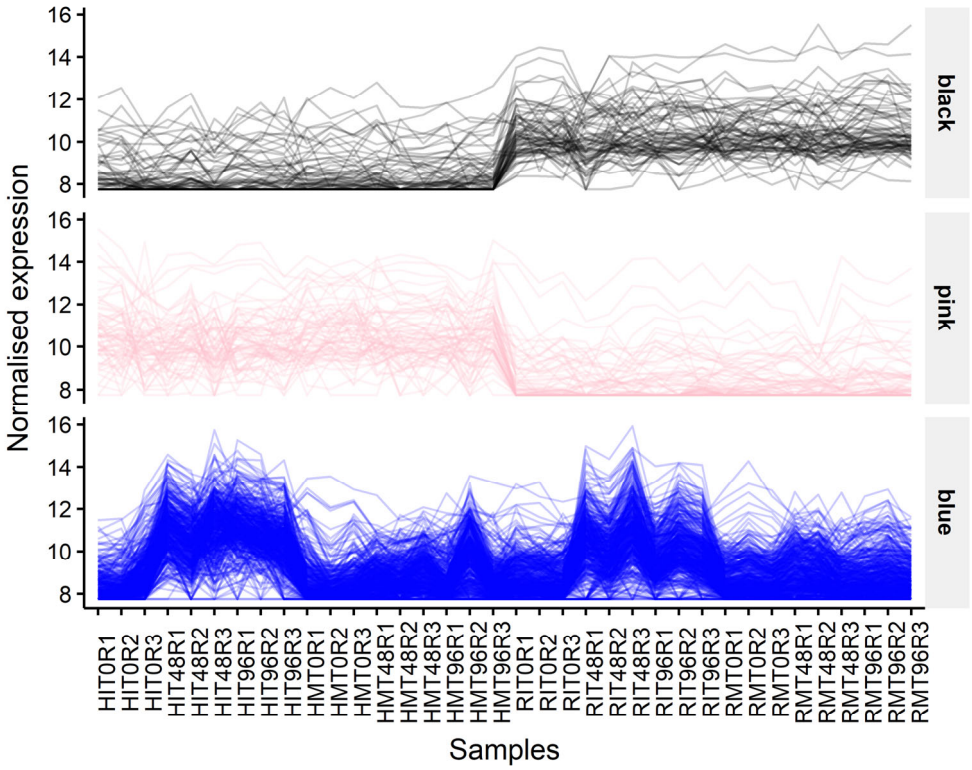

Figure 5. Expression profile of genes in modules associated with *Pyrenophora tritici-repentis* resistant genotype Robigus (black), *P. tritici-repentis* susceptible genotype Hereward (pink), and during pathogen establishment in both genotypes (blue). The x-axis denotes individual RNA-seq samples, labelled by genotype (H = Hereward, R = Robigus), inoculation treatment (I = inoculated, M = mock-inoculated), time point (0, 48, 96 h), and replicate number. The y-axis displays the normalised expression values of transcripts within each module.

By analysing gene significance and module membership ($|GS| > 0.6$ and $MM > 0.8$), 382 transcripts were defined as hub genes (Supplementary Table S2). These can be further assessed in silico or in vivo/vitro for wheat-*Ptr* studies. The expression profile and gene significance of the top 10 hub genes are shown in Figure 6. Transcripts coding for a cysteine protease (putative), sentrin-specific protease (SENP) and a DUF2921 family protein were identified as the top hub gene in the black, pink, and blue modules, respectively, (Supplementary Table S2). Based on our criteria for hub gene recognition, we could identify 59 genes that have high influence in Rob, 46 in Her, and 277 in HerI_RobI (Supplementary Table S2). The highest relative gene expressions were observed in blue module transcripts in Rob, including a thaumatin-like protein (PR-5), chalcone synthase (CHS), and chitinase (Figure 6). Hub genes in black and pink had higher GS values than those from the blue module.

Weighted topological overlap measurements were then used to construct networks representing the mRNA–mRNA interactions in each module (Figures 7a and 8). All networks had high degrees of connectedness between nodes, as expected for hub gene interactomes. Using a force-directed algorithm, the transcripts with higher module membership were positioned in the centre of the networks, illustrating high centrality and connectivity of hubs. Among the hub genes of the blue module (Figure 7a), the top 20 annotations included defence-associated genes: cytochrome P450 (CYPs), 2-oxoglutarate (2OG)/Fe(II)-dependent oxygenase (Fe/2OGs), protein kinases, WRKY transcription factors, pathogenesis-related

(PR) 1, PR-2 (beta-1,3-glucanases), PR-3 (chitinases), PR-4, PR-5, and PR-9 (peroxidases; Figure 7b). Enrichment analysis of gene ontology (GO) cellular components showed that blue module hub genes were mostly components of the plasma membrane and vacuole (Table 2). This indicated that, despite the different levels of resistances to *Ptr* exhibited by Rob and Her, common defence mechanisms were deployed against *Ptr*.

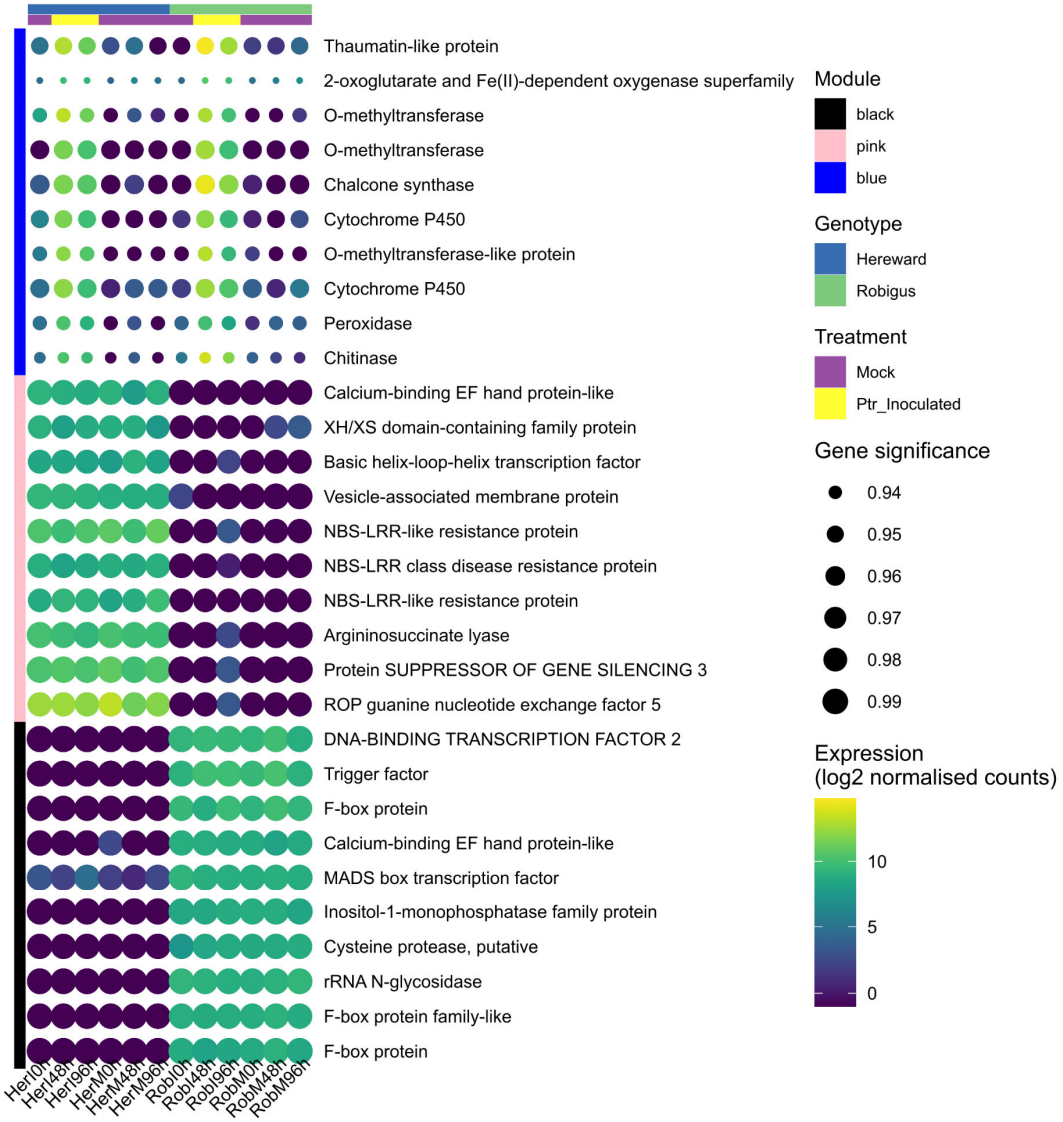

Figure 6. Expression of the top 10 hub genes in blue, pink, and blue modules within transcriptomes of wheat cultivars Robigus (Rob) and Hereward (Her), challenged with *Pyrenophora tritici-repentis* at 0, 48, and 96 h. Also included are data for mock-inoculated Rob and Her plants.

Among the transcripts with highest gene-trait significance (corr > 0.99) in the black module were the following: DNA-binding transcription factor 2, F-box protein, Inositol-1-monophosphatase family protein, trigger factor (TIG), and MADS box transcription factor (Figure 8a). Considering cellular component gene ontologies, plastoglobule, plastid thylakoid, chloroplast stroma, chloroplast thylakoid, plastid stroma, and chloroplast thylakoid membrane protein complex were significantly enriched (FDR < 0.05; Table 2).

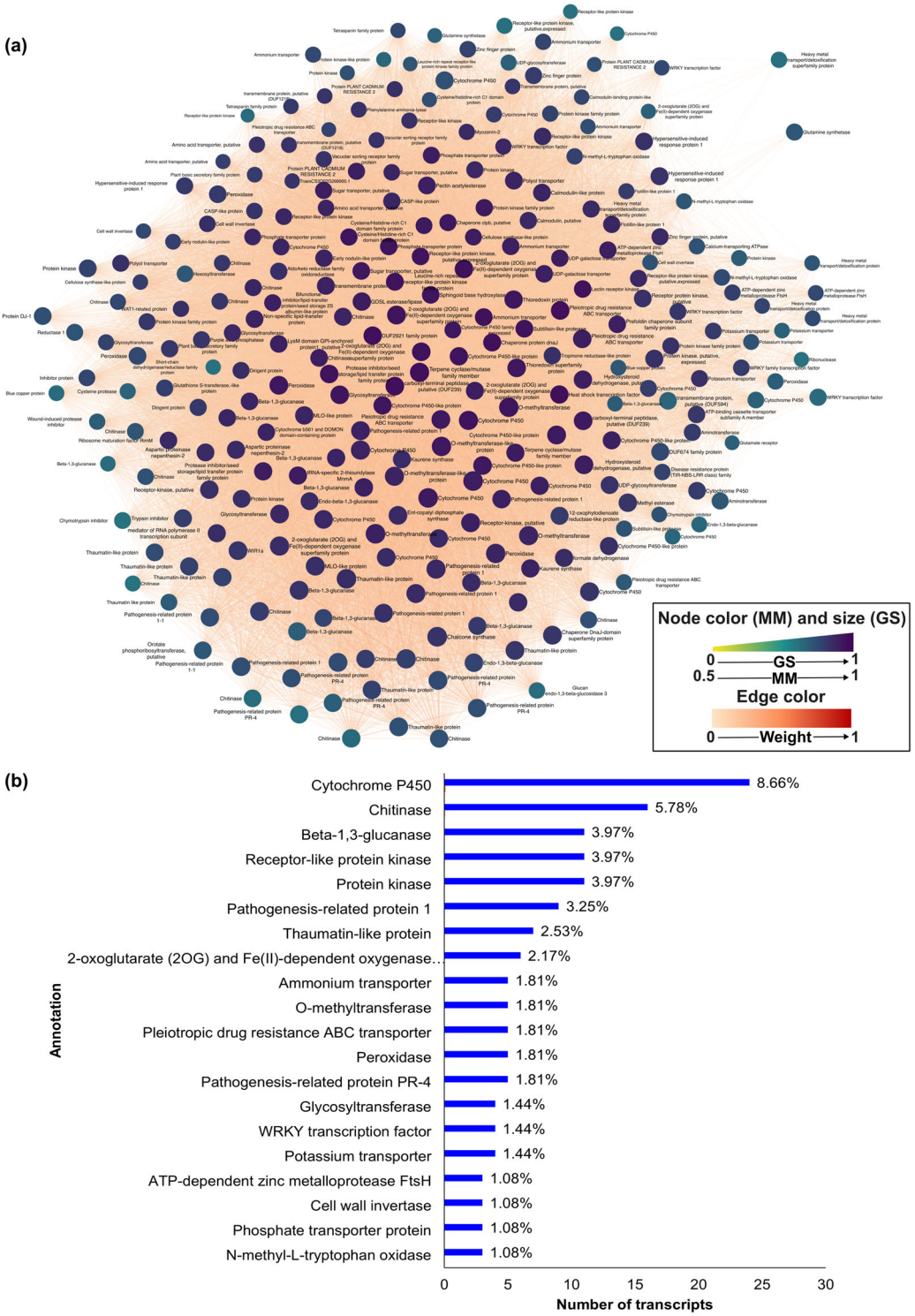

Figure 7. Expression of the top 10 hub genes in blue, pink, and blue modules within transcriptomes of wheat cultivars Robigus (Rob) and Hereward (Her), challenged with *Pyrenophora tritici-repentis* at 0, 48, and 96 h. Also included are data for mock-inoculated Rob and Her plants. Blue module hub (common changes to within transcriptomes of wheat cultivars Robigus [Rob] and Hereward [Her], challenged with *P. tritici-repentis*) (**a**) network and (**b**) summary of top 20 hub gene annotations. Nodes in the network represent individual transcripts, where colour intensity indicates module membership (MM) and node size reflects gene significance (GS). Edge colour and opacity correspond to connection strength (weight values).

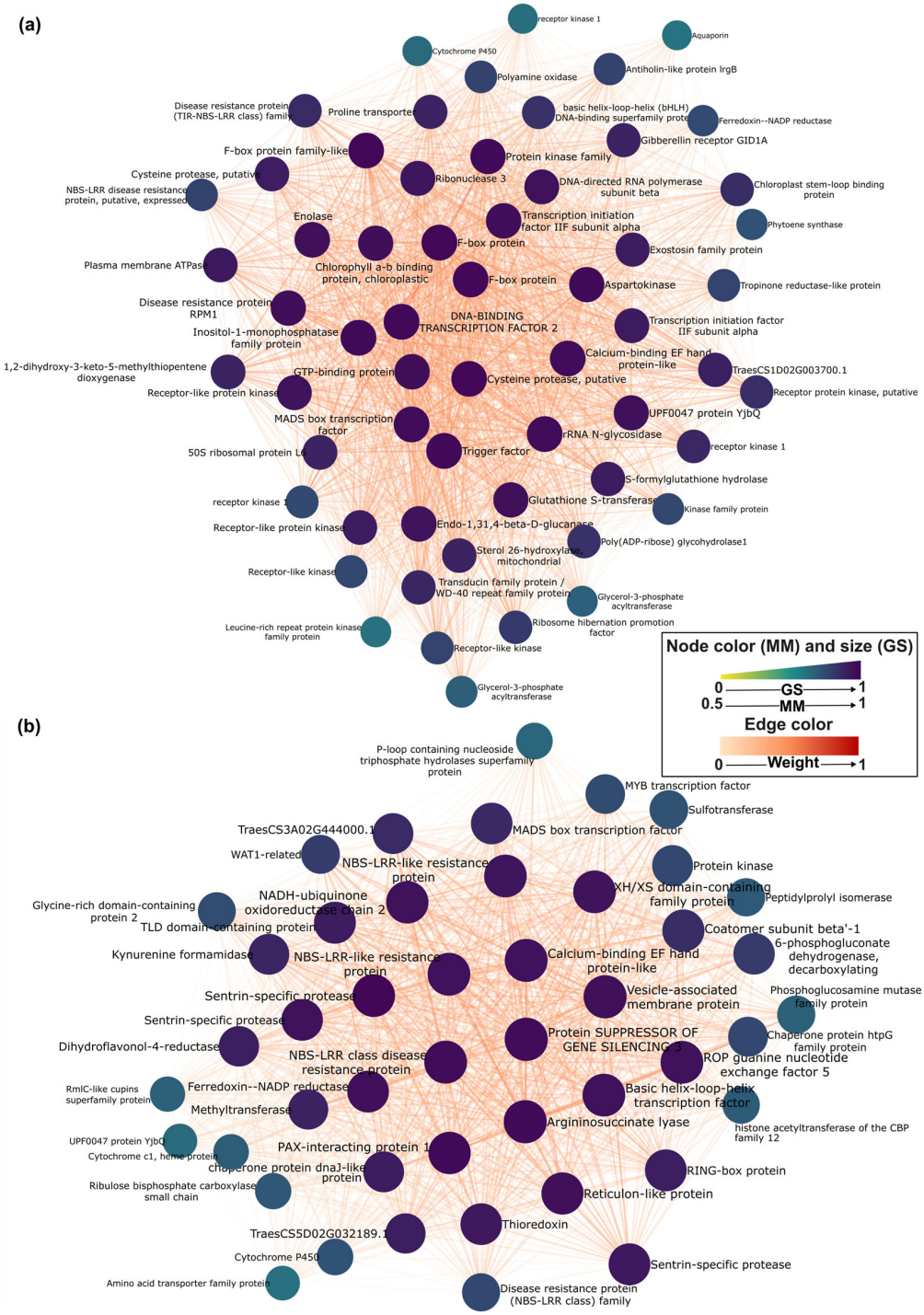

Figure 8. Networks of hub genes in (**a**) black and (**b**) pink modules, respectively, linked to specific transcriptomic changes in wheat cultivars Robigus (Rob) and Hereward (Her), following a challenge with *Pyrenophora tritici-repentis*. Nodes represent individual transcripts, where colour intensity indicates module membership (MM) and node size reflects gene significance (GS). Edge colour and opacity correspond to connection strength (weight values).

Only three transcripts had GS > 0.99 in the pink module, SUPPRESSOR OF GENE SILENCING 3 (SGS3), argininosuccinate lyase, and a vesicle-associated membrane protein (Supplementary Table S2). These three hub genes are in the centre of the network, suggesting that SGS3 is a central gene in the Her genotype (Figure 8b). Interestingly, there are resistance-gene products (nucleotide-binding site (NBS)-leucine rich repeat (LRR) proteins) co-expressed in Her that fail to halt *Ptr* infection, which aligned with the findings from the

blue module. The hub genes in the pink module were not significantly enriched for cellular component gene ontologies.

Table 2. Gene ontology (GO) cellular components significantly enriched with hub genes.

Module	GO Term Name	Term ID	FDR	Num. hubs
blue	intrinsic component of plasma membrane	GO:0031226	6.30×10^{-11}	13
	anchored component of plasma membrane	GO:0046658	9.82×10^{-7}	8
	extracellular region	GO:0005576	2.92×10^{-6}	31
	anchored component of membrane	GO:0031225	9.08×10^{-6}	8
	endoplasmic reticulum lumen	GO:0005788	9.19×10^{-6}	5
	integral component of plasma membrane	GO:0005887	1.07×10^{-4}	5
	intrinsic component of membrane	GO:0031224	2.43×10^{-3}	104
	plasma membrane	GO:0005886	3.26×10^{-3}	19
	plant-type vacuole membrane	GO:0009705	1.61×10^{-2}	3
	plant-type vacuole	GO:0000325	3.89×10^{-2}	3
	integral component of membrane	GO:0016021	3.89×10^{-2}	97
	extracellular space	GO:0005615	4.44×10^{-2}	5
black	plastoglobule	GO:0010287	2.88×10^{-2}	2
	plastid thylakoid	GO:0031976	3.43×10^{-2}	3
	chloroplast stroma	GO:0009570	3.43×10^{-2}	3
	chloroplast thylakoid	GO:0009534	3.43×10^{-2}	3
	plastid stroma	GO:0009532	3.43×10^{-2}	3
	chloroplast thylakoid membrane protein complex	GO:0098807	4.00×10^{-2}	1

4. Discussion

In this study, we used network analysis to elucidate key features of the wheat-tan spot pathosystem that may not have been revealed by our previous transcriptomic–metabolomic analyses [25]. This was an important question, as in the previous study, significant gene expression was targeted by relatively simple fold-change and *t*-test assessments. Such investigations could have missed more complex multivariate/correlative interactions. Using WGCNA, eight groups of co-expressed genes in the genotypes Her (susceptible) and Rob (resistant), either mock-inoculated or challenged with *Ptr*, were observed. This approach identified common defences deployed by both lines upon *Ptr* attack, characterised by genes in the blue module. The black and pink modules were highly correlated (p-value < 0.05) with the resistant and susceptible genotypes, respectively. Transcripts in the black module were found in higher abundance in Rob relative to Her, and the opposite was shown for the pink module. Next, the focus was on hub genes from the black, pink, and blue modules. These could highlight candidate genes and pathways for further study and functional validation (e.g., through gene knockouts, overexpression, or biochemical assays), to confirm their roles in resistance or susceptibility.

4.1. The Blue Module: Pyrenophora Tritici-Repentis Is Likely to Suppress Basal and Effector-Triggered Immunity of Wheat

The shared deployment of defences in interactions leading to disease or moderate resistance raises questions about their functional roles. Both Rob and Her are sensitive to ToxA, as shown by the development of typical necrotic lesions upon *Ptr*, although at different rates [25]. Consequently, expression of common defence responses to *Ptr* infection could be expected, particularly since the time course data were consolidated into single interaction-specific datasets (i.e., RobI and HerI). It should be noted that in Her, these defences may be partially ineffective or manipulated to aid infection.

Wheat–*Ptr* interactions follow an inverse gene-for-gene model, where disease results from the presence of *R* genes in the host that are targeted by the pathogen [42]. In the wheat–*Ptr* pathosystem, this is exemplified by the ToxA and Tsn1 interaction [43]. R genes typically contain a nucleotide-binding site (NBS) leucine-rich repeat (LRR) that mediates effector-triggered immunity (ETI) [44]. *R* gene-like transcripts co-expressed in both lines (1% of blue module) and in the susceptible line (8.7% of pink module) could represent susceptibility factors. The expression of hypersensitive-induced response protein 1 (HIR1) was also triggered by *Ptr* (Supplementary Table S2). HIR1 is a plasma membrane protein associated with defence responses, including localised cell death in rice and barley [45,46], and is known to interact with the receptor-like kinase LRR1 [47,48]. This cell death is likely influenced by ToxA-mediated chloroplast targeting.

Differential expression analysis revealed massive downregulation of chloroplastic proteins and photosynthesis pathways in Her, whereas minor changes occurred in Rob [25]. Our network analysis detected co-expression of three ATP-dependent zinc metalloprotease FtsH genes in both lines, reflecting potential repair mechanisms for ToxA-induced photosynthetic damage. Beyond *R* genes, the broad-spectrum resistance genes *WIR1* (for Wheat Induced Resistance 1) and *MLO*-like (for Mildew resistance locus o) were more highly expressed in response to *Ptr* (Supplementary Table S2). *MLO* functions as a susceptibility factor in barley, aiding host penetration by *B. graminis* f. sp. *hordei* and *M. grisea*. Thus, barley *mlo* recessive lines display resistance [49], whereas *WIR1* exhibits context dependent roles, contributing to resistance in barley and wheat against certain pathogens [50,51]. The elevated expression of *MLO* could influence the relative levels of resistance.

Defence-related genes, including PR proteins, can be activated within 3 h of ToxA exposure [22]. The SnToxA-PR-1 interaction induces necrosis in sensitive wheat, with the phenotype dependent on sustained up-regulation of *PR-1* [52]. While *PR* gene expression commonly promotes resistance, for instance wheat against leaf rust fungus (*Puccinia triticina*) [53,54], salicylic acid (SA)-regulated PR proteins may suppress resistance against necrotrophs [55,56].

Ptr-elicited shifts in the transcription appear to be accompanied by metabolomic changes and are indicated by the activation of key enzymes, such as CYPs, Fe/2OGs, CHS, and PAL (Supplementary Table S2). These enzymes regulate the biosynthesis of cell wall components, hormones, and defence metabolites [57–62]. However, increased expression does not always confer resistance; for example, CHS and PAL activities may correlate with decreased susceptibility or contribute to SA accumulation [63,64], potentially enhancing *Ptr* infection.

4.2. The Blue Module: Pyrenophora Tritici-Repentis Influences Nitrogen Metabolism

Nitrogen (N) is increasingly being recognised as an important player in both defence and disease development in plants. N assimilation can involve a reductase series ($NO_3^- \rightarrow NO_2^- \rightarrow NH_4^+$), followed by transamination to form amino acids, which affects plant development and yield [65]. Increases in applied N can benefit either the host or the pathogen, depending on the pathosystem [66–69]. Our WGCNA showed the co-expression of five ammonium transporters (AMTs), two cytoplasmic glutamine synthases (GLN1/GS1), a glutamate receptor, two aminotransferases, and three amino acid transporters. The preferential expression of AMTs, rather than NO_3^- transporters, could be important, as NH_4^+ induced a higher concentration of most free amino acids than NO_3 [70], and also increased the levels of gamma amino butyric acid (GABA), which serve as a nutrient for the pathogen [71]. A shift towards preferential NH_4^+ assimilation could also reduce the production of nitric oxide, which has important defensive roles [72]. Active transport of amino acids has been shown to increase N levels, photosynthesis, and chlorophylls in Arabidopsis and pea (*Pisum*

sativum) [73–75]. This coordinated regulation of nitrogen metabolism and photosynthetic processes may reflect a compensatory response to ToxA-induced chloroplast stress. In this context, the concurrent expression of FtsH metalloproteases—previously linked to photosystem repair—suggests that the host may attempt to preserve chloroplast function and sustain photosynthesis, despite pathogen-induced damage.

4.3. The Black Module: Defining the Sources Partial Resistance to Pyrenophora Tritici-Repentis in Robigus

GO enrichment analysis showed that resistance in Rob was associated with shifts in transcriptional regulation. Ribonuclease 3 (RNase III), transcription initiation factor IIF subunit alpha (TFIIFα/TFG1), MADS box transcription factor, and DNA-directed RNA polymerase subunit beta (RPB) transcripts were co-expressed in Rob. These maintain RNA homeostasis, including RNA processing, and mediate responses to biotic stress [76–78]. Post-translational modification genes (as shown by the expression of ribosome hibernation promotion factor, rRNA N-glycosidase, trigger factor, DNA-BINDING TRANSCRIPTION FACTOR 2, poly(ADP-ribose), and glycohydrolase 1 (PARG1)), were prominent in the black module. Indeed, 15% of the hub genes in the black module were F-box transcripts. F-box proteins, part of the SCF (SKP1-Cullin-F-box) complex, are widely distributed in the wheat genome [79] and influence disease resistance, among other roles [80,81]. The black module also contained DNA-BINDING TRANSCRIPTION FACTOR 2/SHH2, which is linked to RNA-directed DNA methylation (RdDM) pathways [82–85].

We have recently shown that resistance to *Ptr* in Rob cell wall modification processes lead to increased penetration resistance to *Ptr* infection [25], and this was reflected in the black module. Thus, cell-wall-associated, receptor-like protein kinases, NBS-LRR disease resistance proteins, cellulose synthase, endo-(1,3)(1,4)-beta-D-glucanase, plasma membrane ATPase, antiholin-like protein lrgB, inositol-1-monophosphatase (IMP), and BURP domain protein (RD22) were co-expressed. Cellulose is the main cell wall component and can serve as a physical barrier to phytopathogens [86]. RD22 interacts with cell wall peroxidase, protects cell integrity [87], and is involved in response to stress [88,89]. Inositol-1-monophosphatase play a role in the de novo synthesis of inositol, a lipid involved in cell wall biogenesis, cell-to-cell communication, and hormone signalling [90–92]. Together, these components are likely to be important in the barrier defence against *Ptr* in Rob.

Crucially, our WGCNA approach suggested further resistance mechanisms. Some phytopathogens, including *P. tritici-repentis*, manipulate the chloroplast structures and their functions to assist pathogenicity [93,94]. Our analysis revealed the co-expression of chloroplastic proteins before and during pathogen infection in the resistant genotype. These include chloroplast stem-loop binding protein, chlorophyll a-b binding protein (CAB), phytoene synthase (PSYI), Ferredoxin:NADP+:reductase (FNR), 50S ribosomal large subunit proteins L6 and L28, and GTPase. These proteins are involved in photosynthesis and downstream pathways, and ribosomal assembly and regulation [95–97]. We hypothesise that maintaining a functional chloroplast through expression of structural and regulatory genes in Rob may contribute to resistance to *Ptr*.

4.4. The Pink Module: Changes Associated with Susceptibility in Hereward

In this module, Her susceptibility was linked to transcription regulation, as seen in the overexpression of SGS3, XH/XS domain-containing family protein, PAX-interacting protein 1 (PAXIP1/PTIP), histone acetyltransferase of the CBP family 12 (HAC12) and the transcription factors MADS box, bHLH, and MYB (Figure 8b). SGS3 is a key component of post-transcriptional gene silencing (PTGS) pathways, stabilising double-stranded RNA prior to degradation [98,99]. Its role as a hub in Her suggests that PTGS-related regulation may be important during *Ptr* infection. Similarly, PTIP and HAC12 are involved in

methylation and acetylation processes [100,101], respectively. Their effects have not been investigated in the tan spot pathosystem.

Post-translational modification (PTM)-related transcripts were also found as hub components of the Her network (Figure 8b). Among the genes with PTM functions were a RING-box protein (RBX1) and three SUMO-specific proteases (SENPs), which regulate ubiquitination and SUMOylation processes that control protein stability and turnover [102,103]. Chaperone proteins also play a role in post-translational modifications: most notably, the 70 kDa and 90 kDa heat shock proteins (Hsp70, Hsp90) [104,105], among other roles. In this study, Hsp90 and a DnaJ-like protein (also known as Hsp40, an interacting Hsp70 partner) were found as co-expressing hub genes in the pink module. Cytosolic Hsp70s have been identified as SUMO targets [106], whereas the Hsp90 / Hsp70 complex has been shown to interact with a Cullin-RING ubiquitin ligase (CRL) [107]. The role of ubiquitination/SUMOylation in the susceptible phenotype observed in Her needs to be further investigated.

ROP/RAC GTPases participate in a variety of biological processes which include plant development and hormone responses and are positively regulated by guanine nucleotide exchange factors (ROPGEF) [108–110]. Additionally, ROP GTPases plays a role in auxin signalling [111], membrane trafficking, and cytoskeleton dynamics [112]. Our previous study has pointed to auxin as being a susceptibility factor of wheat to *Ptr*, and polymerisation of the actin cytoskeleton to be a fundamental piece in barrier defences against the tan spot pathogen [25]. Other hub genes included an amino acid/auxin permease (AAAP) transporter, a WAT1-related protein, and a glycine-rich domain-containing protein 2 (GRDP2) (Figure 8b), which may contribute to cellular transport and structural regulation. Altogether, these may indicate a possible role in auxin signalling in susceptibility to *Ptr*.

5. Conclusions

This study used RNA-seq and weighted gene co-expression network analysis (WGCNA) to dissect the molecular responses of wheat to *Ptr* infection. By comparing resistant (Robigus) and susceptible (Hereward) cultivars, we identified distinct gene expression profiles associated with resistance and susceptibility. Notably, the resistant cultivar showed increased expression of chloroplast ribosomal genes and transcriptional regulators, whereas the susceptible line exhibited elevated levels of post-transcriptional and translational modifiers. We identified 59 hub genes in modules associated with resistance and 46 hub genes in modules linked to susceptibility. Many of these genes had not been previously associated with the wheat–*Ptr* pathosystem, highlighting the added value of network-based analyses for discovering novel components of plants' immune responses. Experimental validation of the identified hub genes will be essential to fully uncover their roles and potential for breeding disease-resistant wheat varieties.

Supplementary Materials: The following supporting information can be downloaded at: https://www.mdpi.com/article/10.3390/microbiolres16110242/s1. Figure S1: Phenotypic characterisation of wheat cultivars (a) Robigus (Rob) and (b) Hereward (Her) at 336 h post inoculation with *Pyrenophora tritici-repentis*. Scale bar = 1 cm; Figure S2: A scatterplot of gene significance vs. module membership of transcripts in modules relevant for (a) tan spot-resistant wheat cultivar Robigus (Rob), (b) tan spot-susceptible wheat cultivar Hereward (Her), (c) and pathogen elicited within transcriptomes of both cultivars when challenged with *Pyrenophora tritici-repentis*. Correlation values are denoted as "cor", and *p*-value as "*p*"; Table S1: Weighted correlation network analysis (WGCNA) of RNA-seq data; Table S2: Detailed result of intramodular analysis, hub genes network attributes and annotation.

Author Contributions: Conceptualization, L.C.F., F.M.S., and L.A.J.M.; methodology, L.C.F.; formal analysis, L.C.F.; data curation, L.C.F.; writing—original draft preparation, L.C.F.; writing—review and editing, L.C.F., F.M.S., and L.A.J.M.; funding acquisition, F.M.S. and L.A.J.M. All authors have read and agreed to the published version of the manuscript.

Funding: LCF acknowledges the support of the AberDoc PhD and IBERS scholarships, Aberystwyth University.

Institutional Review Board Statement: Not applicable.

Informed Consent Statement: Not applicable.

Data Availability Statement: The datasets analysed during the current study are available in the GitHub repository, https://github.com/lcferr/wheat-Ptr-WGCNA (accessed on 31 January 2025).

Conflicts of Interest: The authors declare no conflicts of interest.

Abbreviations

The following abbreviations are used in this manuscript:

Ptr	*Pyrenophora tritici-repentis*
hpi	Hours post inoculation
Rob	Robigus
Her	Hereward
corr	Correlation
ME	Module eigengene
GS	Gene significance
MM	Module membership
FDR	False discovery rate

References

1. Ciuffetti, L.M.; Manning, V.A.; Pandelova, I.; Faris, J.D.; Friesen, T.L.; Strelkov, S.E.; Weber, G.L.; Goodwin, S.B.; Wolpert, T.J.; Figueroa, M. *Pyrenophora tritici-repentis*: A Plant Pathogenic Fungus with Global Impact. *Genom. Plant-Assoc. Fungi Monocot Pathog.* **2014**, 1–39. [CrossRef]
2. Mironenko, N.; Krämer, I.; Ordon, F.; Mikhailova, L.; Kopahnke, D.; Timopheeva, E. Intraspecific Genetic Diversity of *Pyrenophora tritici-repentis* (Died.) Drechs. (*Drechslera tritici-repentis* [Died.] Shoem.) Detected by Random Amplified Polymorphic DNA Assays. *Arch. Phytopathol. Plant Prot.* **2007**, *40*, 431–440. [CrossRef]
3. Sautua, F.J.; Carmona, M.A. Detection and Characterization of QoI Resistance in *Pyrenophora tritici-repentis* Populations Causing Tan Spot of Wheat in Argentina. *Plant Pathol.* **2021**, *70*, 2125–2136. [CrossRef]
4. Singh, R.P.; Singh, P.K.; Rutkoski, J.; Hodson, D.P.; He, X.; Jørgensen, L.N.; Hovmøller, M.S.; Huerta-Espino, J. Disease Impact on Wheat Yield Potential and Prospects of Genetic Control. *Annu. Rev. Phytopathol.* **2016**, *54*, 303–322. [CrossRef]
5. Lamari, L.; Bernier, C.C. Toxin of Pyrenophora Tritici-Repentis: Host-Specificity, Significance in Disease, and Inheritance of Host Reaction. *Phytopathology* **1989**, *79*, 740. [CrossRef]
6. Faris, J.D.; Anderson, J.A.; Francl, L.J.; Jordahl, J.G. Chromosomal Location of a Gene Conditioning Insensitivity in Wheat to a Necrosis-Inducing Culture Filtrate from Pyrenophora Tritici-Repentis. *Phytopathology* **1996**, *86*, 459–463. [CrossRef]
7. Effertz, R.J.; Meinhardt, S.W.; Anderson, J.A.; Jordahl, J.G.; Francl, L.J. Identification of a Chlorosis-Inducing Toxin from *Pyrenophora tritici-repentis* and the Chromosomal Location of an Insensitivity Locus in Wheat. *Phytopathology* **2007**, *92*, 527–533. [CrossRef] [PubMed]
8. Friesen, T.; Faris, J. Molecular Mapping of Resistance to *Pyrenophora tritici-repentis* Race 5 and Sensitivity to Ptr ToxB in Wheat. *Theor. Appl. Genet.* **2004**, *109*, 464–471. [CrossRef]
9. Faris, J.D.; Liu, Z.; Xu, S.S. Genetics of Tan Spot Resistance in Wheat. *Theor. Appl. Genet.* **2013**, *126*, 2197–2217. [CrossRef]
10. Lamari, L.; Sayoud, R.; Boulif, M.; Bernier, C.C. Identification of a New Race in Pyrenophora Tritici-Repentis: Implications for the Current Pathotype Classification System. *Can. J. Plant Pathol.* **1995**, *17*, 312–318. [CrossRef]
11. Ali, S.; Francl, L.J. A New Race of *Pyrenophora tritici-repentis* from Brazil. *Plant Dis.* **2002**, *86*, 1050. [CrossRef]
12. Lamari, L.; Strelkov, S.E.; Yahyaoui, A.; Orabi, J.; Smith, R.B. The Identification of Two New Races of *Pyrenophora tritici-repentis* from the Host Center of Diversity Confirms a One-to-One Relationship in Tan Spot of Wheat. *Phytopathology* **2003**, *93*, 391–396. [CrossRef]
13. McDonald, M.C.; Ahren, D.; Simpfendorfer, S.; Milgate, A.; Solomon, P.S. The Discovery of the Virulence Gene ToxA in the Wheat and Barley Pathogen *Bipolaris sorokiniana*. *Mol. Plant Pathol.* **2018**, *19*, 432–439. [CrossRef]

14. Friesen, T.L.; Stukenbrock, E.H.; Liu, Z.; Meinhardt, S.; Ling, H.; Faris, J.D.; Rasmussen, J.B.; Solomon, P.S.; McDonald, B.A.; Oliver, R.P. Emergence of a New Disease as a Result of Interspecific Virulence Gene Transfer. *Nat. Genet.* **2006**, *38*, 953–956. [CrossRef]
15. Oliver, R.P.; Friesen, T.L.; Faris, J.D.; Solomon, P.S. Stagonospora Nodorum: From Pathology to Genomics and Host Resistance. *Annu. Rev. Phytopathol.* **2011**, *50*, 23–43. [CrossRef] [PubMed]
16. Manning, V.A.; Ciuffetti, L.M. Localization of Ptr ToxA Produced by *Pyrenophora tritici-repentis* Reveals Protein Import into Wheat Mesophyll Cells. *Plant Cell* **2005**, *17*, 3203–3212. [CrossRef] [PubMed]
17. Manning, V.A.; Hardison, L.K.; Ciufetti, L.M. Ptr ToxA Interacts with a Chloroplast-Localized Protein. *Mol. Plant-Microbe Interact.* **2007**, *20*, 168–177. [CrossRef] [PubMed]
18. Manning, V.A.; Hamilton, S.M.; Karplus, P.A.; Ciuffetti, L.M. The Arg-Gly-Asp-Containing, Solvent-Exposed Loop of Ptr ToxA Is Required for Internalization. *Mol. Plant-Microbe Interact.* **2008**, *21*, 315–325. [CrossRef]
19. Manning, V.A.; Andrie, R.M.; Trippe, A.F.; Ciuffetti, L.M. Ptr ToxA Requires Multiple Motifs for Complete Activity. *Mol. Plant-Microbe Interact.* **2004**, *17*, 491–501. [CrossRef]
20. Manning, V.A.; Chu, A.L.; Steeves, J.E.; Wolpert, T.J.; Ciuffetti, L.M. A Host-Selective Toxin of Pyrenophora Tritici- Repentis, Ptr ToxA, Induces Photosystem Changes and Reactive Oxygen Species Accumulation in Sensitive Wheat. *Mol. Plant-Microbe Interact.* **2009**, *22*, 665–676. [CrossRef] [PubMed]
21. Pandelova, I.; Betts, M.F.; Manning, V.A.; Wilhelm, L.J.; Mockler, T.C.; Ciuffetti, L.M. Analysis of Transcriptome Changes Induced by Ptr ToxA in Wheat Provides Insights into the Mechanisms of Plant Susceptibility. *Mol. Plant* **2009**, *2*, 1067–1083. [CrossRef] [PubMed]
22. Pandelova, I.; Figueroa, M.; Wilhelm, L.J.; Manning, V.A.; Mankaney, A.N.; Mockler, T.C.; Ciuffetti, L.M. Host-Selective Toxins of *Pyrenophora tritici-repentis* Induce Common Responses Associated with Host Susceptibility. *PLoS ONE* **2012**, *7*, e40240. [CrossRef] [PubMed]
23. Andersen, E.J.; Nepal, M.P.; Ali, S. Necrotrophic Fungus *Pyrenophora tritici-repentis* Triggers Expression of Multiple Resistance Components in Resistant and Susceptible Wheat Cultivars. *Plant Pathol. J.* **2021**, *37*, 99. [CrossRef] [PubMed]
24. Ferreira, L.C.; Santana, F.M.; Beckmann, M.; Mur, L.A.J. Using MAGIC against Tan Spot Disease: How Multiparent Advanced Generation Intercross Wheat Lines Respond to *Pyrenophora tritici-repentis* Infection. *Phytopathology* **2020**, *110*, S2.94–S2.95. [CrossRef]
25. Ferreira, L.; Santana, F.; Scagliusi, S.; Beckmann, M.; Mur, L. Omic Characterisation of Multi-Component Defences against the Necrotrophic Pathogen *Pyrenophora tritici-repentis* in Wheat. *Plant Biol.* **2025**, *27*, 347–361. [CrossRef]
26. Mackay, I.J.; Bansept-Basler, P.; Barber, T.; Bentley, A.R.; Cockram, J.; Gosman, N.; Greenland, A.J.; Horsnell, R.; Howells, R.; O'Sullivan, D.M.; et al. An Eight-Parent Multiparent Advanced Generation Inter-Cross Population for Winter-Sown Wheat: Creation, Properties, and Validation. *G3 Genes Genomes Genet.* **2014**, *4*, 1603–1610. [CrossRef]
27. Yan, J.; Risacher, S.L.; Shen, L.; Saykin, A.J. Network Approaches to Systems Biology Analysis of Complex Disease: Integrative Methods for Multi-Omics Data. *Brief. Bioinform.* **2018**, *19*, 1370–1381. [CrossRef]
28. van Dam, S.; Võsa, U.; van der Graaf, A.; Franke, L.; de Magalhães, J.P. Gene Co-Expression Analysis for Functional Classification and Gene–Disease Predictions. *Brief. Bioinform.* **2018**, *19*, 575–592. [CrossRef]
29. Pandaranayaka, E.P.; Frenkel, O.; Elad, Y.; Prusky, D.; Harel, A. Network Analysis Exposes Core Functions in Major Lifestyles of Fungal and Oomycete Plant Pathogens. *BMC Genomics* **2019**, *20*, 1020. [CrossRef]
30. Cheng, C.-H.; Shen, B.-N.; Shang, Q.-W.; Liu, L.-Y.D.; Peng, K.-C.; Chen, Y.-H.; Chen, F.-F.; Hu, S.-F.; Wang, Y.-T.; Wang, H.-C.; et al. Gene-to-Gene Network Analysis of the Mediation of Plant Innate Immunity by the Eliciting Plant Response-Like 1 (Epl1) Elicitor of Trichoderma Formosa. *Mol. Plant-Microbe Interact.* **2018**, *31*, 683–691. [CrossRef]
31. Hu, Q.; Tan, L.; Gu, S.; Xiao, Y.; Xiong, X.; Zeng, W.; Feng, K.; Wei, Z.; Deng, Y. Network Analysis Infers the Wilt Pathogen Invasion Associated with Non-Detrimental Bacteria. *NPJ Biofilms Microbiomes* **2020**, *6*, 8. [CrossRef]
32. Zhang, B.; Horvath, S. A General Framework for Weighted Gene Co-Expression Network Analysis. *Stat. Appl. Genet. Mol. Biol.* **2005**, *4*. [CrossRef]
33. Li, Y.; Pearl, S.A.; Jackson, S.A. Gene Networks in Plant Biology: Approaches in Reconstruction and Analysis. *Trends Plant Sci.* **2015**, *20*, 664–675. [CrossRef]
34. Langfelder, P.; Horvath, S. WGCNA: An R Package for Weighted Correlation Network Analysis. *BMC Bioinform.* **2008**, *9*, 559. [CrossRef]
35. Zhang, H.; Fu, Y.; Guo, H.; Zhang, L.; Wang, C.; Song, W.; Yan, Z.; Wang, Y.; Ji, W. Transcriptome and Proteome-Based Network Analysis Reveals a Model of Gene Activation in Wheat Resistance to Stripe Rust. *Int. J. Mol. Sci.* **2019**, *20*, 1106. [CrossRef]
36. Love, M.I.; Huber, W.; Anders, S. Moderated Estimation of Fold Change and Dispersion for RNA-Seq Data with DESeq2. *Genome Biol.* **2014**, *15*, 550. [CrossRef]

37. Shannon, P.; Markiel, A.; Ozier, O.; Baliga, N.S.; Wang, J.T.; Ramage, D.; Amin, N.; Schwikowski, B.; Ideker, T. Cytoscape: A Software Environment for Integrated Models of Biomolecular Interaction Networks. *Genome Res.* **2003**, *13*, 2498. [CrossRef] [PubMed]
38. Appels, R.; Eversole, K.; Feuillet, C.; Keller, B.; Rogers, J.; Stein, N.; Pozniak, C.J.; Stein, N.; Choulet, F.; Distelfeld, A.; et al. Shifting the Limits in Wheat Research and Breeding Using a Fully Annotated Reference Genome. *Science* **2018**, *361*, eaar7191. [CrossRef] [PubMed]
39. Ramírez-González, R.H.; Borrill, P.; Lang, D.; Harrington, S.A.; Brinton, J.; Venturini, L.; Davey, M.; Jacobs, J.; Van Ex, F.; Pasha, A.; et al. The Transcriptional Landscape of Polyploid Wheat. *Science* **2018**, *361*, eaar6089. [CrossRef]
40. Maere, S.; Heymans, K.; Kuiper, M. BiNGO: A Cytoscape Plugin to Assess Overrepresentation of Gene Ontology Categories in Biological Networks. *Bioinformatics* **2005**, *21*, 3448–3449. [CrossRef] [PubMed]
41. Merico, D.; Isserlin, R.; Stueker, O.; Emili, A.; Bader, G.D. Enrichment Map: A Network-Based Method for Gene-Set Enrichment Visualization and Interpretation. *PLoS ONE* **2010**, *5*, e13984. [CrossRef] [PubMed]
42. Fenton, A.; Antonovics, J.; Brockhurst, M.A. Inverse-Gene-for-Gene Infection Genetics and Coevolutionary Dynamics. *Am. Nat.* **2009**, *174*, E230–E242. [CrossRef] [PubMed]
43. Faris, J.D.; Zhang, Z.; Lu, H.; Lu, S.; Reddy, L.; Cloutier, S.; Fellers, J.P.; Meinhardt, S.W.; Rasmussen, J.B.; Xu, S.S.; et al. A Unique Wheat Disease Resistance-like Gene Governs Effector-Triggered Susceptibility to Necrotrophic Pathogens. *Proc. Natl. Acad. Sci. USA* **2010**, *107*, 13544–13549. [CrossRef]
44. Jones, J.D.G.; Dangl, J.L. The Plant Immune System. *Nature* **2006**, *444*, 323–329. [CrossRef]
45. Nadimpalli, R.; Yalpani, N.; Johal, G.S.; Simmons, C.R. Prohibitins, Stomatins, and Plant Disease Response Genes Compose a Protein Superfamily That Controls Cell Proliferation, Ion Channel Regulation, and Death. *J. Biol. Chem.* **2000**, *275*, 29579–29586. [CrossRef]
46. Rostoks, N.; Schmierer, D.; Kudrna, D.; Kleinhofs, A. Barley Putative Hypersensitive Induced Reaction Genes: Genetic Mapping, Sequence Analyses and Differential Expression in Disease Lesion Mimic Mutants. *Theor. Appl. Genet.* **2003**, *107*, 1094–1101. [CrossRef]
47. Zhou, L.; Cheung, M.Y.; Zhang, Q.; Lei, C.L.; Zhang, S.H.; Sun, S.S.M.; Lam, H.M. A Novel Simple Extracellular Leucine-Rich Repeat (ELRR) Domain Protein from Rice (OsLRR1) Enters the Endosomal Pathway and Interacts with the Hypersensitive-Induced Reaction Protein 1 (OsHIR1). *Plant Cell Environ.* **2009**, *32*, 1804–1820. [CrossRef]
48. Zhou, L.; Cheung, M.Y.; Li, M.W.; Fu, Y.; Sun, Z.; Sun, S.M.; Lam, H.M. Rice Hypersensitive Induced Reaction Protein 1 (OsHIR1) Associates with Plasma Membrane and Triggers Hypersensitive Cell Death. *BMC Plant Biol.* **2010**, *10*, 290. [CrossRef]
49. Jarosch, B.; Kogel, K.H.; Schaffrath, U. The Ambivalence of the Barley Mlo Locus: Mutations Conferring Resistance Against Powdery Mildew (*Blumeria graminis* f. sp. *hordei*) Enhance Susceptibility to the Rice Blast Fungus *Magnaporthe grisea*. *Mol. Plant-Microbe Interact.* **2007**, *12*, 508–514. [CrossRef]
50. Douchkov, D.; Johrde, A.; Nowara, D.; Himmelbach, A.; Lueck, S.; Niks, R.; Schweizer, P. Convergent Evidence for a Role of WIR1 Proteins during the Interaction of Barley with the Powdery Mildew Fungus *Blumeria graminis*. *J. Plant Physiol.* **2011**, *168*, 20–29. [CrossRef] [PubMed]
51. Tufan, H.A.; Mcgrann, G.R.D.; Maccormack, R.; Boyd, L.A. TaWIR1 Contributes to Post-Penetration Resistance to Magnaporthe Oryzae, but Not *Blumeria graminis* f. Sp. Tritici, in Wheat. *Mol. Plant Pathol.* **2012**, *13*, 653–665. [CrossRef]
52. Lu, S.; Faris, J.D.; Sherwood, R.; Friesen, T.L.; Edwards, M.C. A Dimeric PR-1-Type Pathogenesis-Related Protein Interacts with ToxA and Potentially Mediates ToxA-Induced Necrosis in Sensitive Wheat. *Mol. Plant Pathol.* **2014**, *15*, 650–663. [CrossRef]
53. Gao, L.; Wang, S.; Li, X.Y.; Wei, X.J.; Zhang, Y.J.; Wang, H.Y.; Liu, D.Q. Expression and Functional Analysis of a Pathogenesis-Related Protein 1 Gene, TcLr19PR1, Involved in Wheat Resistance Against Leaf Rust Fungus. *Plant Mol. Biol. Report.* **2015**, *33*, 797–805. [CrossRef]
54. Zhang, J.; Wang, F.; Liang, F.; Zhang, Y.; Ma, L.; Wang, H.; Liu, D. Functional Analysis of a Pathogenesis-Related Thaumatin-like Protein Gene TaLr35PR5 from Wheat Induced by Leaf Rust Fungus. *BMC Plant Biol.* **2018**, *18*, 76. [CrossRef] [PubMed]
55. Wang, B.; Sun, Y.; Song, N.; Zhao, M.; Liu, R.; Feng, H.; Wang, X.; Kang, Z. *Puccinia striiformis* f. sp. *tritici* MicroRNA-like RNA 1 (Pst-MilR1), an Important Pathogenicity Factor of *Pst*, Impairs Wheat Resistance to *Pst* by Suppressing the Wheat Pathogenesis-Related 2 Gene. *New Phytol.* **2017**, *215*, 338–350. [CrossRef]
56. Sanaz Ramezanpour, S.; Mohammadi, M.; Navabpour, S.; Soltanloo, H.; Kia, S.; Kalateh Arabi, M. Study on Expression Pattern of Chalcone Synthase And-1,3-Glucanase under Septoria Tritici Treatment in Wheat by Quantitative Real Time PCR. *J. Agric. Environ. Sci.* **2012**, *12*, 1431–1436. [CrossRef]
57. Xu, J.; Wang, X.Y.; Guo, W.Z. The Cytochrome P450 Superfamily: Key Players in Plant Development and Defense. *J. Integr. Agric.* **2015**, *14*, 1673–1686. [CrossRef]
58. Nomura, T.; Ishihara, A.; Iwamura, H.; Endo, T.R. Molecular Characterization of Benzoxazinone-Deficient Mutation in Diploid Wheat. *Phytochemistry* **2007**, *68*, 1008–1016. [CrossRef]

59. Pandian, B.A.; Sathishraj, R.; Djanaguiraman, M.; Prasad, P.V.V.; Jugulam, M. Role of Cytochrome P450 Enzymes in Plant Stress Response. *Antioxidants* **2020**, *9*, 454. [CrossRef]
60. Saito, K.; Kobayashi, M.; Gong, Z.; Tanaka, Y.; Yamazaki, M. Direct Evidence for Anthocyanidin Synthase as a 2-Oxoglutarate-Dependent Oxygenase: Molecular Cloning and Functional Expression of CDNA from a Red Forma of Perilla Frutescens. *Plant J.* **1999**, *17*, 181–189. [CrossRef]
61. Mitchell, A.J.; Weng, J.K. Unleashing the Synthetic Power of Plant Oxygenases: From Mechanism to Application. *Plant Physiol.* **2019**, *179*, 813. [CrossRef] [PubMed]
62. Hahlbrock, K.; Grisebach, H. Enzymic Controls in the Biosynthesis of Lignin and Flavonoids. *Ann. Rev. Plant Physiol.* **1979**, *30*, 105–130. [CrossRef]
63. Chen, Z.; Zheng, Z.; Huang, J.; Lai, Z.; Fan, B. Biosynthesis of Salicylic Acid in Plants. *Plant Signal Behav.* **2009**, *4*, 493–496. [CrossRef] [PubMed]
64. Ortuño, A.; Díaz, L.; Alvarez, N.; Porras, I.; García-Lidón, A.; Del Río, J.A. Comparative Study of Flavonoid and Scoparone Accumulation in Different Citrus Species and Their Susceptibility to *Penicillium digitatum*. *Food Chem.* **2011**, *125*, 232–239. [CrossRef]
65. Marschner, H. General Introduction to the Mineral Nutrition of Plants. In *Inorganic Plant Nutrition*; Springer: Berlin/Heidelberg, Germany, 1983; pp. 5–60. [CrossRef]
66. Mur, L.A.J.; Simpson, C.; Kumari, A.; Gupta, A.K.; Gupta, K.J. Moving Nitrogen to the Centre of Plant Defence against Pathogens. *Ann. Bot.* **2017**, *119*, 703–709. [CrossRef] [PubMed]
67. Sun, Y.; Wang, M.; Mur, L.A.J.; Shen, Q.; Guo, S. Unravelling the Roles of Nitrogen Nutrition in Plant Disease Defences. *Int. J. Mol. Sci.* **2020**, *21*, 572. [CrossRef]
68. Devadas, R.; Simpfendorfer, S.; Backhouse, D.; Lamb, D.W. Effect of Stripe Rust on the Yield Response of Wheat to Nitrogen. *Crop J.* **2014**, *2*, 201–206. [CrossRef]
69. Brennan, R.F. The Role of Manganese and Nitrogen Nutrition in the Susceptibility of Wheat Plants to Take-All in Western Australia. *Fertil. Res.* **1992**, *31*, 35–41. [CrossRef]
70. Huber, D.M.; Tsai, C.Y. Influence of the Form of Nitrogen on Ammonium, Amino Acids and N-assimelating Enzyme Activity in Maize Genotypes 1. *J. Plant Nutr.* **2008**, *18*, 747–763. [CrossRef]
71. Mead, O.; Thynne, E.; Winterberg, B.; Solomon, P.S. Characterising the Role of GABA and Its Metabolism in the Wheat Pathogen Stagonospora Nodorum. *PLoS ONE* **2013**, *8*, e78368. [CrossRef]
72. Gupta, K.J.; Brotman, Y.; Segu, S.; Zeier, T.; Zeier, J.; Persijn, S.T.; Cristescu, S.M.; Harren, F.J.M.; Bauwe, H.; Fernie, A.R.; et al. The Form of Nitrogen Nutrition Affects Resistance against *Pseudomonas syringae* Pv. phaseolicola in Tobacco. *J. Exp. Bot.* **2013**, *64*, 553–568. [CrossRef]
73. Zhang, L.; Tan, Q.; Lee, R.; Trethewy, A.; Lee, Y.H.; Tegeder, M. Altered Xylem-Phloem Transfer of Amino Acids Affects Metabolism and Leads to Increased Seed Yield and Oil Content in Arabidopsis. *Plant Cell* **2010**, *22*, 3603–3620. [CrossRef]
74. Perchlik, M.; Tegeder, M. Leaf Amino Acid Supply Affects Photosynthetic and Plant Nitrogen Use Efficiency under Nitrogen Stress. *Plant Physiol.* **2018**, *178*, 174–188. [CrossRef]
75. Perchlik, M.; Tegeder, M. Improving Plant Nitrogen Use Efficiency through Alteration of Amino Acid Transport Processes. *Plant Physiol.* **2017**, *175*, 235–247. [CrossRef]
76. MacIntosh, G.C.; Castandet, B. Organellar and Secretory Ribonucleases: Major Players in Plant RNA Homeostasis1[OPEN]. *Plant Physiol.* **2020**, *183*, 1438–1452. [CrossRef]
77. Olmedo, G.; Guzmán, P. Processing Precursors with RNase III in Plants. *Plant Sci.* **2008**, *175*, 741–746. [CrossRef]
78. Gan, J.; Shaw, G.; Tropea, J.E.; Waugh, D.S.; Court, D.L.; Ji, X. A Stepwise Model for Double-Stranded RNA Processing by Ribonuclease III. *Mol. Microbiol.* **2008**, *67*, 143–154. [CrossRef] [PubMed]
79. Hong, M.J.; Kim, J.B.; Seo, Y.W.; Kim, D.Y. F-Box Genes in the Wheat Genome and Expression Profiling in Wheat at Different Developmental Stages. *Genes* **2020**, *11*, 1154. [CrossRef] [PubMed]
80. Li, H.; Wei, C.; Meng, Y.; Fan, R.; Zhao, W.; Wang, X.; Yu, X.; Laroche, A.; Kang, Z.; Liu, D. Identification and Expression Analysis of Some Wheat F-Box Subfamilies during Plant Development and Infection by *Puccinia triticina*. *Plant Physiol. Biochem.* **2020**, *155*, 535–548. [CrossRef]
81. Stefanowicz, K.; Lannoo, N.; Van Damme, E.J.M. Plant F-Box Proteins—Judges between Life and Death. *Crit. Rev. Plant Sci.* **2015**, *34*, 523–552. [CrossRef]
82. Law, J.A.; Vashisht, A.A.; Wohlschlegel, J.A.; Jacobsen, S.E. SHH1, a Homeodomain Protein Required for DNA Methylation, as Well as RDR2, RDM4, and Chromatin Remodeling Factors, Associate with RNA Polymerase IV. *PLoS Genet.* **2011**, *7*, e1002195. [CrossRef] [PubMed]
83. Haag, J.R.; Brower-Toland, B.; Krieger, E.K.; Sidorenko, L.; Nicora, C.D.; Norbeck, A.D.; Irsigler, A.; LaRue, H.; Brzeski, J.; McGinnis, K.; et al. Functional Diversification of Maize RNA Polymerase IV and V Subtypes via Alternative Catalytic Subunits. *Cell Rep.* **2014**, *9*, 378–390. [CrossRef]

84. Zhang, H.; Ma, Z.Y.; Zeng, L.; Tanaka, K.; Zhang, C.J.; Ma, J.; Bai, G.; Wang, P.; Zhang, S.W.; Liu, Z.W.; et al. DTF1 Is a Core Component of RNA-Directed DNA Methylation and May Assist in the Recruitment of Pol IV. *Proc. Natl. Acad. Sci. USA* **2013**, *110*, 8290–8295. [CrossRef]
85. Wang, Y.; Zhou, X.; Luo, J.; Lv, S.; Liu, R.; Du, X.; Jia, B.; Yuan, F.; Zhang, H.; Du, J. Recognition of H3K9me1 by Maize RNA-Directed DNA Methylation Factor SHH2. *J. Integr. Plant Biol.* **2021**, *63*, 1091–1096. [CrossRef]
86. Menna, A.; Dora, S.; Sancho-Andrés, G.; Kashyap, A.; Meena, M.K.; Sklodowski, K.; Gasperini, D.; Coll, N.S.; Sánchez-Rodríguez, C. A Primary Cell Wall Cellulose-Dependent Defense Mechanism against Vascular Pathogens Revealed by Time-Resolved Dual Transcriptomics. *BMC Biol.* **2021**, *19*, 161. [CrossRef]
87. Wang, H.; Zhou, L.; Fu, Y.; Cheung, M.Y.; Wong, F.L.; Phang, T.H.; Sun, Z.; Lam, H.M. Expression of an Apoplast-Localized BURP-Domain Protein from Soybean (GmRD22) Enhances Tolerance towards Abiotic Stress. *Plant Cell Environ.* **2012**, *35*, 1932–1947. [CrossRef]
88. Ding, X.; Hou, X.; Xie, K.; Xiong, L. Genome-Wide Identification of BURP Domain-Containing Genes in Rice Reveals a Gene Family with Diverse Structures and Responses to Abiotic Stresses. *Planta* **2009**, *230*, 149–163. [CrossRef] [PubMed]
89. Xu, H.; Li, Y.; Yan, Y.; Wang, K.; Gao, Y.; Hu, Y. Genome-Scale Identification of Soybean BURP Domain-Containing Genes and Their Expression under Stress Treatments. *BMC Plant Biol.* **2010**, *10*, 197. [CrossRef]
90. Nourbakhsh, A.; Collakova, E.; Gillaspy, G.E. Characterization of the Inositol Monophosphatase Gene Family in Arabidopsis. *Front. Plant Sci.* **2015**, *5*, 725. [CrossRef]
91. Sharma, N.; Chaudhary, C.; Khurana, P. Wheat Myo-Inositol Phosphate Synthase Influences Plant Growth and Stress Responses via Ethylene Mediated Signaling. *Sci. Rep.* **2020**, *10*, 10766. [CrossRef] [PubMed]
92. Levine, E.E.; Frank Loewus, B.A.; Kelly, S.; Neufeldt, E.F. Metabolism of myo-inositol in plants: Conversion to pectin, hemicellulose, D-xylose, and sugar acids. *Proc. Natl. Acad. Sci. USA* **1962**, *48*, 421. [CrossRef]
93. Lu, Y.; Yao, J. Chloroplasts at the Crossroad of Photosynthesis, Pathogen Infection and Plant Defense. *Int. J. Mol. Sci.* **2018**, *19*, 3900. [CrossRef]
94. Yang, F.; Xiao, K.; Pan, H.; Liu, J. Chloroplast: The Emerging Battlefield in Plant–Microbe Interactions. *Front. Plant Sci.* **2021**, *12*, 218. [CrossRef]
95. Morales, R.; Charon, M.H.; Kachalova, G.; Serre, L.; Medina, M.; Gómez-Moreno, C.; Frey, M. A Redox-Dependent Interaction between Two Electron-Transfer Partners Involved in Photosynthesis. *EMBO Rep.* **2000**, *1*, 271. [CrossRef] [PubMed]
96. Goss, T.; Hanke, G. The End of the Line: Can Ferredoxin and Ferredoxin NADP(H) Oxidoreductase Determine the Fate of Photosynthetic Electrons? *Curr. Protein Pept. Sci.* **2014**, *15*, 385. [CrossRef]
97. Jeon, Y.; Ahn, C.S.; Jung, H.J.; Kang, H.; Park, G.T.; Choi, Y.; Hwang, J.; Pai, H.S. DER Containing Two Consecutive GTP-Binding Domains Plays an Essential Role in Chloroplast Ribosomal RNA Processing and Ribosome Biogenesis in Higher Plants. *J. Exp. Bot.* **2014**, *65*, 117–130. [CrossRef]
98. Fukunaga, R.; Doudna, J.A. DsRNA with 5′ Overhangs Contributes to Endogenous and Antiviral RNA Silencing Pathways in Plants. *EMBO J.* **2009**, *28*, 545–555. [CrossRef]
99. Mourrain, P.; Béclin, C.; Elmayan, T.; Feuerbach, F.; Godon, C.; Morel, J.B.; Jouette, D.; Lacombe, A.M.; Nikic, S.; Picault, N.; et al. Arabidopsis SGS2 and SGS3 Genes Are Required for Posttranscriptional Gene Silencing and Natural Virus Resistance. *Cell* **2000**, *101*, 533–542. [CrossRef]
100. Cho, Y.W.; Hong, T.; Hong, S.H.; Guo, H.; Yu, H.; Kim, D.; Guszczynski, T.; Dressler, G.R.; Copeland, T.D.; Kalkum, M.; et al. PTIP Associates with MLL3- and MLL4-Containing Histone H3 Lysine 4 Methyltransferase Complex. *J. Biol. Chem.* **2007**, *282*, 20395–20406. [CrossRef] [PubMed]
101. Sterner, D.E.; Berger, S.L. Acetylation of Histones and Transcription-Related Factors. *Microbiol. Mol. Biol. Rev.* **2000**, *64*, 435. [CrossRef]
102. Kim, J.H.; Baek, S.H. Emerging Roles of Desumoylating Enzymes. *Biochim. Et Biophys. Acta (BBA)—Mol. Basis Dis.* **2009**, *1792*, 155–162. [CrossRef]
103. Gray, W.M.; Hellmann, H.; Dharmasiri, S.; Estelle, M. Role of the Arabidopsis RING-H2 Protein RBX1 in RUB Modification and SCF Function. *Plant Cell* **2002**, *14*, 2137. [CrossRef]
104. Nitika; Porter, C.M.; Truman, A.W.; Truttmann, M.C. Post-Translational Modifications of Hsp70 Family Proteins: Expanding the Chaperone Code. *J. Biol. Chem.* **2020**, *295*, 10689–10708. [CrossRef] [PubMed]
105. Backe, S.J.; Sager, R.A.; Woodford, M.R.; Makedon, A.M.; Mollapour, M. Post-Translational Modifications of Hsp90 and Translating the Chaperone Code. *J. Biol. Chem.* **2020**, *295*, 11099–11117. [CrossRef]
106. Sharma, M.; Fuertes, D.; Perez-Gil, J.; Lois, L.M. SUMOylation in Phytopathogen Interactions: Balancing Invasion and Resistance. *Front. Cell Dev. Biol.* **2021**, *9*, 2189. [CrossRef]
107. Ehrlich, E.S.; Wang, T.; Luo, K.; Xiao, Z.; Niewiadomska, A.M.; Martinez, T.; Xu, W.; Neckers, L.; Yu, X.F. Regulation of Hsp90 Client Proteins by a Cullin5-RING E3 Ubiquitin Ligase. *Proc. Natl. Acad. Sci. USA* **2009**, *106*, 20330–20335. [CrossRef]
108. Yang, Z.; Fu, Y. ROP/RAC GTPase Signaling. *Curr. Opin. Plant Biol.* **2007**, *10*, 490–494. [CrossRef] [PubMed]

109. Nagawa, S.; Xu, T.; Yang, Z. RHO GTPase in Plants: Conservation and Invention of Regulators and Effectors. *Small GTPases* **2010**, *1*, 78. [CrossRef] [PubMed]
110. Berken, A.; Thomas, C.; Wittinghofer, A. A New Family of RhoGEFs Activates the Rop Molecular Switch in Plants. *Nature* **2005**, *436*, 1176–1180. [CrossRef] [PubMed]
111. Wu, H.-m.; Hazak, O.; Cheung, A.Y.; Yalovsky, S. RAC/ROP GTPases and Auxin Signaling. *Plant Cell* **2011**, *23*, 1208–1218. [CrossRef]
112. Yalovsky, S.; Bloch, D.; Sorek, N.; Kost, B. Regulation of Membrane Trafficking, Cytoskeleton Dynamics, and Cell Polarity by ROP/RAC GTPases. *Plant Physiol.* **2008**, *147*, 1527–1543. [CrossRef] [PubMed]